Head to head domain wall structures in thin magnetic strips

R. D. McMichael and M. J. Donahue
National Institute of Standards and Technology,
Gaithersburg, MD 20899

Abstract—**We present calculations of head to head domain wall structures in magnetic strips of $Ni_{80}Fe_{20}$ with widths, w, ranging from 75 nm to 500 nm and thicknesses, t, from 1 nm to 64 nm. Neglecting magnetocrystalline and magnetostrictive anisotropy energies, minimization of exchange and magnetostatic energy leads to one of two types of domain wall structures: 'transverse' walls with magnetization at the center of the wall directed transverse to the strip axis and 'vortex' walls where the magnetization forms a vortex at the center of the wall. Calculation of the domain wall energies leads to a proposed phase diagram for head to head domain walls where transverse walls have lower energy when dimensions are less than $t_{\rm crit} w_{\rm crit} \approx 130 A/\mu_0 M_s^2$.**

I. Introduction

In recent years, the ability to fabricate submicron features in magnetic films has opened a new field of experimental micromagnetics, with considerable interest in submicron magnetic strips [1], [2]. A carefully calculated phase diagram of domain wall structures in thin magnetic strips has been published by Ramstöck et al. describing the low-energy domain wall configurations for domain walls running parallel to the length of the strip [3]. In that calculation, the magnetization was constrained to be uniform along the length of the strip.

The lowest energy state in an infinitely long magnetic strip is a uniformly magnetized state. The next highest energy stable state will be a configuration having two semi-infinite uniform domains and a localized head-to-head domain wall with an associated finite total energy. In contrast, a two-domain state with a 180° domain wall running parallel to the strip edges will have infinite energy, due to the finite energy per unit length of the domain wall.

From a practical standpoint, head-to-head domain walls play a role in magnetization reversal in thin strips where the remanent state has domain structures at the ends of the strip [4]–[7], and magnetization switches through propagation of head-to-head domain structures from the ends through the sample [1], [6].

In this paper we calculate head-to-head domain structures that form at the boundary between two oppositely directed, semi-infinite domains in magnetic strips.

Manuscript received Jan 30, 1997.

R. D. McMichael, e-mail rmcmichael@nist.gov

II. Calculation Method

Our calculation involves solution of Brown's equations by finite-differences on a 2D square grid. At the grid points, the magnetization is represented by 3D vectors, $\mathbf{m}_i$, having unit length. Only the magnetostatic energy and the exchange energy are taken into account. Other anisotropy terms (magnetocrystalline, magnetostrictive, etc.) are set to zero for simplicity. Because only magnetostatic and exchange energy terms are considered, the relevant length scales that are involved in the problem are the the thickness, t, of the film, the width, w, of the patterned strip of film, and the magnetostatic exchange length, $\delta = (A/\mu_0 M_s^2)^{1/2}$, which is the relevant length scale for vortex cores.

A general solution to this problem would be best described in terms of the dimensionless variables w/δ and t/δ. However, for concreteness, the calculations were performed using parameters appropriate for $Ni_{80}Fe_{20}$, $A = 1.3 \times 10^{-11}$J/m and $M_s = 8.0 \times 10^5$A/m, giving $\delta = 4.0$ nm.

We discretize the infinite strip using a square grid over a region with a length, $l = 4w$, as illustrated in Fig. 1. Inside the discretized region, the magnetization is constrained to be uniform through the thickness of the film. Outside the gridded region, the magnetization is constrained to lie along the length of the strip, directed inward towards the gridded region. The magnetostatic fields of the semi-infinite strip ends are replaced by fields due to plates of positive magnetostatic charge at each end of the gridded region.

This discretization scheme has a range of validity that is limited by the requirement that the energy of vortices in the thin film strips be calculated correctly. Therefore, the discretization must be fine enough that vortex cores can be resolved. This limitation is felt most strongly in calculations of wide strips, where a large number of cells is needed, and calculations proceed very slowly. An additional limitation is that having uni-

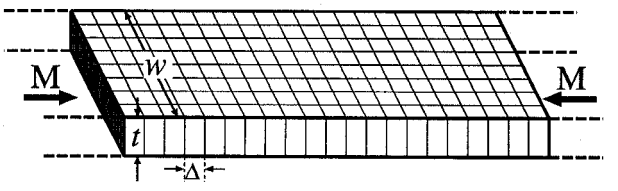

Fig. 1. Schematic of discretization scheme for head-to-head domain walls in an infinite strip. The shaded area represents a ribbon of magnetostatic charge used to represent the magnetostatic effects of the infinitely long ends of the strip.

form magnetization through the strip thickness must not be an overly restrictive assumption. While a full 3D model would be needed to confirm this assumption, the results of the 2D calculation, to be shown below, contain Néel-like transitions, and symmetric Néel walls have been shown to possess only weak z-dependence of the magnetization [3].

Minimization of the energy is achieved by following heavily damped Landau-Lifshitz-Gilbert equations of motion,

$$\frac{d\mathbf{m}}{dt} = -\gamma(\mathbf{m} \times \mathbf{H}_{\text{eff}}) - \gamma\lambda\mathbf{m} \times (\mathbf{m} \times \mathbf{H}_{\text{eff}}). \quad (1)$$

This ODE is solved numerically using a second order predictor-corrector technique. The step size, dt, is adjusted as necessary to insure that the total energy decreases at each step. The iteration is continued until the maximum torque over all of the spins in the system is below a threshold value. At this point, as a stability check, the spins are given random 2° perturbations, and the ODE iteration is restarted. The process of perturbation and ODE solving is repeated until successive solutions yield energies within a given tolerance.

Magnetostatic fields are calculated separately for fields in the x-y plane of the sample and for fields directed out of the plane of the sample in the z direction. For fields in the x-y plane, $H^{\text{D}}_{x,y}$, we calculate the magnetostatic charge, $\rho = -\nabla \cdot \mathbf{M}$, assuming constant ρ over grid cells [8]. The magnetostatic potential due to a single cell with unit charge is calculated by numerical integration and the potential is then calculated over the whole grid with a fast Fourier transform convolution technique. To isolate the calculation region from periodic 'images' (induced by the cyclic nature of FFT-based convolution), the 'sample' grid is embedded in a zero-padded 2 × 2 larger grid [9]. Finally, $H^{\text{D}}_{x,y}$, is determined by numerical differentiation of the magnetostatic potential [8].

The z-component of the magnetostatic field, H^{D}_z, is calculated directly from the values of m_z on the grid. The field due to surface charges on a single block of z-directed magnetization is integrated numerically and a zero-padded Fourier transform convolution is used to determine H^{D}_z throughout the grid.

The exchange energy was calculated using equal magnitude dot-product interactions with spins at the eight nearest neighbor sites [10]. This form of the exchange energy is equivalent to assuming that the magnetization in a cell is determined from the values of $\mathbf{m}$ on grid points at the corners of the cell through a bilinear interpolation.

III. Results

We used two basic initial states in the calculations, an abrupt head-to-head transition and one with a block of out-of-plane spins in the transition region. Both of these states included random perturbations of 2° for each spin. In almost all cases, these initial conditions led to one of two types of head-to-head domain walls: a 'transverse' wall, illustrated in Fig. 2a, or a 'vortex' wall illustrated in Fig. 2b.

The transverse wall has a reflection symmetry about a line perpendicular to the strip axis. Note that in Fig. 2a, the wall

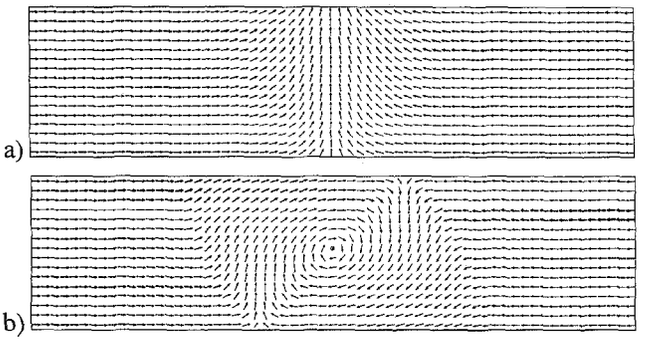

Fig. 2. a) 'Transverse' domain structure for a head-to-head wall calculated in a 2 nm thick, 250 nm wide strip of $Ni_{80}Fe_{20}$, and b) 'vortex' domain structure for a head-to-head wall calculated in a 32 nm thick, 250 nm wide strip of $Ni_{80}Fe_{20}$. Each arrow represents the magnetization of a subsample from a 4x4 cell block.

appears wider at the top edge of the strip than at the bottom edge. This asymmetry is quite prominent in the wider strips, where the transverse wall appears as a triangular, transversely oriented domain bounded on two sides by a "V" configuration of 45° Néel walls oriented diagonally to the strip axis.

The vortex structure has a two-fold rotational symmetry about its center point, and bears a striking resemblance to the structure observed experimentally in a cobalt strip [1]. In the the wider strips, the dominant feature of the vortex wall is a Néel wall running diagonally across the strip, with a vortex at its center. For the thickest films, and depending on initial conditions, we have occasionally observed two vortices and a cross-tie wall in the central region of the vortex wall.

In some instances, the system obtained a lower energy by sliding the domain wall to one end of the gridded region. To prevent this, the domain walls were stabilized by the application of a field of amplitude $0.1M_s$ to a few spins in the central region of the sample, either transverse or perpendicular to the strip for transverse or vortex wall calculations, respectively. This stabilization field contributed less than 0.5% to the total wall energy.

We have calculated domain wall energy for the two types of walls as a function of film thickness for a number of strip widths, and the results are presented in Fig. 3. For each type of wall, calculations were carried out as a function of t for w = 75 nm, 125 nm, 250 nm, and 500 nm. The final state for each thickness was used as an initial condition for the next value of t. Calculations of vortex wall energies started at large t with initial out-of-plane transitions, and calculations of transverse wall energies started at low t with initial abrupt transitions. For each strip width there is a considerable range of thickness for dual stability, but it is not clear how much of this range is due to our use of a stabilization field as described above.

As a partial phase diagram for head to head walls in thin magnetic strips, the crossover points in Fig. 3 are plotted in Fig. 4 in terms of the dimensionless strip thickness t/δ and width w/δ. Transverse domain walls have lower energy than vortex walls for low values of t and w, and the crossover critical dimensions suggest a phase boundary of the form

$$t \cdot w = C\delta^2. \quad (2)$$

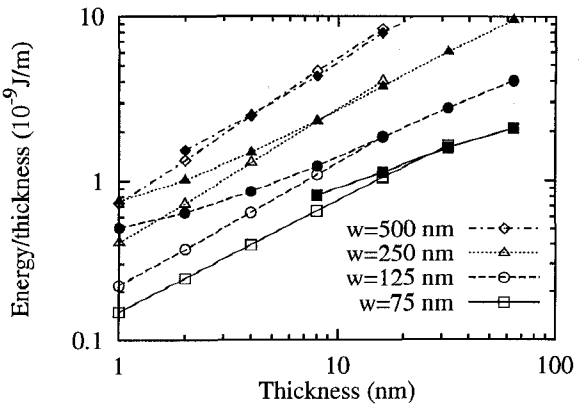

Fig. 3. Domain wall energy as a function of film thickness for head-to-head walls with transverse (open symbols) and vortex structures (filled symbols) in strips of $Ni_{80}Fe_{20}$ with widths of 75 nm, 125 nm, 250 nm, and 500 nm.

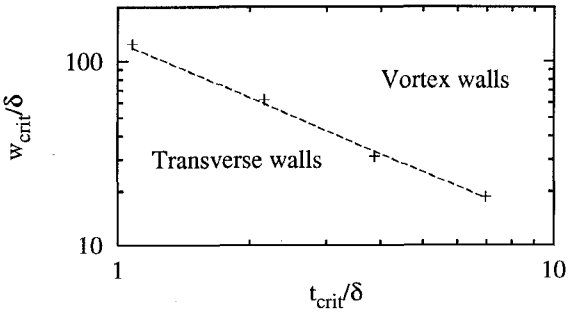

Fig. 4. Partial phase diagram of head to head domain wall structures in thin magnetic strips. δ is the magnetostatic exchange length.

The dashed line in Fig. 4 corresponds to C = 128.

IV. Discussion

The energy associated with both the transverse and vortex walls comes predominantly from magnetostatics, but in a vortex domain wall the exchange energy contribution is more significant. For example, in a w=250 nm, t=8 nm strip, where the total energies are very nearly equal, the transverse wall energy is 93% magnetostatic and 7% exchange, while the vortex wall energy is 78% magnetostatic and 22% exchange.

The phase boundary can be estimated by considering the differences in the exchange and magnetostatic energies of features that appear in the calculated domain patterns. An estimate of the exchange energy difference is the energy of a vortex, which appears in the vortex wall but not in the transverse wall:

$$(E_{\text{vortex}} - E_{\text{trans}})_{\text{ex}} \approx 2\pi t A \ln\left(\frac{r_{\max}}{r_{\min}}\right), \qquad (3)$$

where $r_{\max}$ is the outer radius of the vortex, on the order of a Néel wall width or the strip width, and $r_{\min}$ is the radius of the vortex core, on the order of δ.

An estimate of the magnetostatic energy difference is the magnetostatic energy associated with magnetization oriented perpendicular to the strip edge, which occurs in transverse walls, and to a much lesser degree in vortex walls. For **M** perpendicular to the strip edge, the resulting magnetostatic field has a maximum magnitude of $\frac{1}{2}M_s$ at the edge, and falls to $\frac{1}{4}M_s$ at a distance of $t/2$ from the edge. Taking this half-maximum value of the field as an average value in the region within a distance t of the edge, and integrating over a volume with a length $\approx w$, The magnetostatic energy from edge directed magnetization is then estimated to be

$$(E_{\text{vortex}} - E_{\text{trans}})_{\text{ms}} \approx -\frac{1}{2}\int_{\text{V}} \mu_0 \mathbf{H}\cdot\mathbf{M} \approx -\frac{1}{8}\mu_0 M_s^2 t^2 w. \qquad (4)$$

To find the phase boundary, the sum of the exchange and magnetostatic energy differences given in (3) and (4) is set equal to zero. The resulting expression for the phase boundary is

$$wt = 16\pi \ln\left(\frac{r_{\max}}{r_{\min}}\right)\delta^2. \qquad (5)$$

The maximum and minimum dimensions of the vortex, $r_{\max}$ and $r_{\min}$, are determined by the material parameters and perhaps by sample geometry. Taking $r_{\max} = w/2$ and $r_{\min} = \delta$ with $w/\delta \approx 40$ gives $C = 150$. Given the weak logarithmic dependence on $r_{\max}$ and $r_{\min}$ and the approximations in (3) and (4), the agreement with the computational results in (2) is quite good.

References

[1] M. Rührig, B. Khamsepour, K. J. Kirk, J. N. Chapman, P. Aitchison, S. McVitie, and C. D. W. Wilkinson, "The fabrication and Magnetic Properties of Acicular Magnetic Nano-Elements," *IEEE Trans. MAG*, vol. 32, pp. 4452-4457, Sept. 1996.

[2] S. Y. Chou, M. Wei, P. R. Krauss, and P. B. Fischer, "Study of nanoscale magnetic structures fabricated using electron-beam lithography and quantum magnetic disk," *J. Vac. Sci. Technol. B*, vol. 12, pp. 3695-3698, Nov./Dec. 1994.

[3] K. Ramstock, W. Hartung, and A. Hubert, "The Phase Diagram of Domain Walls in Narrow Magnetic Stripes," *Phys. Stat. Sol. (a)*, vol. 155, pp. 505-516, June 1996.

[4] Jason Gadbois and Jian-Gang Zhu, "Effect of Edge Roughness in Nano-Scale Magnetic Bar Switching," *IEEE Trans. MAG*, vol. 31, pp. 3802-3804, Nov. 1995.

[5] Samuel W. Yuan, H. Neal Bertram, Joseph F. Smyth, and Sheldon Schultz, "Size Effects of Switching Fields of Thin Permalloy Particles," *IEEE Trans. MAG*, vol. 28, pp. 3171-3173 Sept. 1992.

[6] Jeffery McCord, Alex Hubert, Gerold Schröpfer and Uwe Loreit, "Domain Observation on Magnetoresistive Sensor Elements," *IEEE Trans. MAG*, vol. 32, pp. 4806-4808, Sept. 1996.

[7] Round-robin results for a $2 \times 1 \times .02$ μm $Ni_{80}Fe_{20}$ computational problem are available from
http://cobalt.nist.gov/mumag/prob1/prob1report.html.

[8] D. V. Berkov, K. Ramstöck, and A. Hubert, "Solving Micromagnetic Problems: Towards an Optimal Numerical Method," *Phys. Stat. Sol. (a)*, vol. 137, pp. 207-225, May 1993.

[9] T. G. Stockham, "High Speed Convolution and Correlation," *Joint Computer Conference Proceedings*, vol. 28, pp. 229-233, 1966.

[10] M. J. Donahue and R. D. McMichael, "Exchange energy representations in computational micromagnetics," *Physica B, in press.*